Article

Benzoxazine Oligomers: Evidence for a Helical Structure from Solid-State NMR Spectroscopy and DFT-Based Dynamics and Chemical Shift Calculations

Gillian R. Goward, Daniel Sebastiani, Ingo Schnell, Hans Wolfgang Spiess, Ho-Dong Kim, and Hatsuo Ishida

J. Am. Chem. Soc., **2003**, 125 (19), 5792-5800• DOI: 10.1021/ja029059r • Publication Date (Web): 22 April 2003

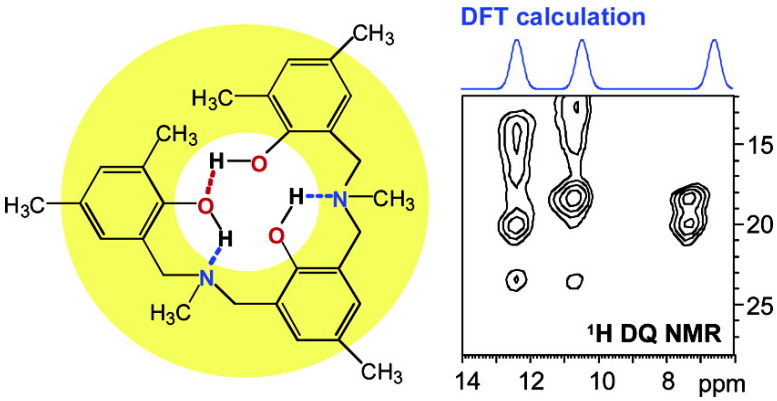

More About This Article

Additional resources and features associated with this article are available within the HTML version:

- Supporting Information
- Links to the 6 articles that cite this article, as of the time of this article download
- Access to high resolution figures
- Links to articles and content related to this article
- Copyright permission to reproduce figures and/or text from this article

View the Full Text HTML

J|A|C|S
ARTICLES
Published on Web 04/22/2003

Benzoxazine Oligomers: Evidence for a Helical Structure from Solid-State NMR Spectroscopy and DFT-Based Dynamics and Chemical Shift Calculations

Gillian R. Goward,[†,§] Daniel Sebastiani,[†] Ingo Schnell,[†] Hans Wolfgang Spiess,*[,†] Ho-Dong Kim,[‡] and Hatsuo Ishida[‡]

Contribution from the Max-Planck-Institut für Polymerforschung, Postfach 3148, D-55021 Mainz, Germany, and Department of Chemistry, Case Western Reserve University, 10900 Euclid Avenue, Cleveland, Ohio 44106-7078

Received October 23, 2002; E-mail: spiess@mpip-mainz.mpg.de

Abstract: A combination of molecular modeling, DFT calculations, and advanced solid-state NMR experiments is used to elucidate the supramolecular structure of a series of benzoxazine oligomers. Intramolecular hydrogen bonds are characterized and identified as the driving forces for ring-shape and helical conformations of trimeric and tetrameric units. In fast MAS ^{1}H NMR spectra, the resonances of the protons forming the hydrogen bonds can be assigned and used for validating and refining the structure by means of DFT-based geometry optimizations and ^{1}H chemical-shift calculations. Also supporting these proposed structures are homonuclear ^{1}H−^{1}H double-quantum NMR spectra, which identify the local proton−proton proximities in each material. Additionally, quantitative ^{15}N−^{1}H distance measurements obtained by analysis of dipolar spinning sideband patterns confirm the optimized geometry of the tetramer. These results clearly support the predicted helical geometry of the benzoxazine polymer. This geometry, in which the N···H···O and O···H···O hydrogen bonds are protected on the inside of the helix, can account for many of the exemplary chemical properties of the polybenzoxazine materials. The combination of advanced experimental solid-state NMR spectroscopy with computational geometry optimizations, total energy, and NMR spectra calculations is a powerful tool for structural analysis. Its results provide significantly more confidence than the individual measurements or calculations alone, in particular, because the microscopic structure of many disordered systems cannot be elucidated by means of conventional methods due to lack of long-range order.

Introduction

Supramolecular structures often suffer from a lack of long-range crystallinity, due to the comparatively weak interactions that determine their structures, for example, hydrogen bonding[1−7] and π-stacking.[8−10] Solid-state NMR, however, does not require long-range ordering to provide structural details of these fascinating systems. Hydrogen bonding and π-stacking are building blocks of supramolecular interactions and show up clearly in high-resolution solid-state ^{1}H NMR studies.[11−13] The powerful combination of quantum chemical calculations with experimental NMR studies has been used previously to elucidate structural details of other supramolecular systems.[14−16] Here we apply a combination of molecular modeling, density functional theory (DFT) calculations, and experimental measurements to obtain insight into the structure of a series of benzoxazine oligomers and to show that hydrogen bonds have a strong influence on the structural conformation that is adopted.

Supramolecular structures influenced by self-assembly and hydrogen bonding are also frequently observed in polymeric architectures.[17−21] Polybenzoxazines are a classic example of

[†] Max-Planck-Institut für Polymerforschung.
[‡] Case Western Reserve University.
[§] Current address: Department of Chemistry, McMaster University, Hamilton ON, Canada.

(1) Jeffery, G. A.; Saenger, W. *Hydrogen Bonding in Biological Structures*; Springer-Verlag: New York, 1991.
(2) Sijbesma, R. P.; Beijer, F. H.; Brunsveld, L.; Folmer, B. J.; Hirschberg, J. H.; Lange, R. F.; Lowe, J. K.; Meijer, E. W. *Science* **1997**, *278*, 1601−1604.
(3) Lehn, J. M. *Science* **1993**, *260*, 1762−1763.
(4) Brunsveld, L.; Folmer, B. J.; Meijer, E. W.; Sijbesma, R. P. *Chem. Rev.* **2001**, *101*, 4071−4098.
(5) Schmuck, C. W. W. *Angew. Chem., Int. Ed.* **2001**, *40*, 4363.
(6) Brunsveld, L.; Vekemans, J. A.; Hirschberg, J. H.; Sijbesma, R. P.; Meijer, E. W. *Proc. Natl. Acad. Sci. U.S.A.* **2002**, *99*, 4977−4982.
(7) Yamauchi, K.; Lizotte, J. R.; Hercules, D. M.; Vergne, M. J.; Long, T. E. *J. Am. Chem. Soc.* **2002**, *124*, 8599−8604.
(8) Ajayaghosh, A.; George, S. J. *J. Am. Chem. Soc.* **2001**, *123*, 5148−5149.
(9) Lahiri, S.; Thompson, J. L.; Moore, J. S. *J. Am. Chem. Soc.* **2000**, *122*, 11315−11319.
(10) Brown, S. P.; Schnell, I.; Brand, J. D.; Müllen, K.; Spiess, H. W. *J. Am. Chem. Soc.* **1999**, *121*, 6712−6718.
(11) Percec, V.; Glodde, M.; Bera, T. K.; Miura, Y.; Shiyanovskaya, I.; Singer, K. D.; Balagurusamy, V. S.; Heiney, P. A.; Schnell, I.; Rapp, A.; Spiess, H. W.; Hudson, S. D.; Duan, H. *Nature* **2002**, *419*, 384−387.
(12) Brown, S. P.; Spiess, H. W. *Chem. Rev.* **2001**, *101*, 4125−4156.
(13) Wei Y.; McDermott, A. *ACS Symp. Ser.* **1999**, *732*, 177−193.
(14) Ochsenfeld, C.; Head-Gordon, M. *Chem. Phys. Lett.* **1997**, *270*, 399−405.
(15) Ochsenfeld, C. *Phys. Chem. Chem. Phys.* **2000**, *2*, 2153−2159.
(16) Ochsenfeld, C.; Brown, S. P.; Schnell, I.; Gauss, J.; Spiess, H. W. *J. Am. Chem. Soc.* **2001**, *123*, 2597−2606.
(17) Percec, V.; Ahn, C. H.; Ungar, G.; Yeardley, D. J. P.; Moller, M.; Sheiko, S. S. *Nature* **1998**, *391*, 161−164.
(18) Berl, V.; Schmutz, M.; Krische, M. J.; Khoury, R. G.; Lehn, J. M. *Chemistry* **2002**, *8*, 1227−1244.
(19) Chino, K.; Ashiura, M. *Macromolecules* **2001**, *34*, 9201−9204.

10.1021/ja029059r CCC: $25.00

such a structure. Polybenzoxazines exhibit a number of unusual properties, including low volumetric shrinkage or expansion upon curing,[22] lack of water absorption and excellent resistance to chemicals and UV light,[23,24] as well as surprisingly high T_g values given the low cross-linking density,[25] all of which make them attractive candidates for many commercial applications. These properties have been attributed to the unique hydrogen-bonding structure found in these materials, and therefore this property has been the focus of recent investigation. In particular, extensive crystallographic, NMR, and IR studies of the dimer precursors have provided much insight.[26,27] However, the benzoxazine dimers organize themselves in a highly regular, paired lattice; hence the model cannot be extended to account for the unique properties of the parent polymer. Therefore, synthetic efforts were made to procure other oligomers of the benzoxazine material and thereby bridge the gap between the fully determined dimer structure and the unknown polymer structure.[28] The objective here is to improve our understanding of the polymer architecture, through studies of the hydrogen bonding in the oligomers, and thereby understand the remarkable physical characteristics of the polymers. In this paper, we focus on the methyl-substituted benzoxazine trimer and tetramer, which cannot be investigated by conventional X-ray diffraction techniques, because suitable crystals could not be prepared. From the trimer, it might be possible to obtain crystallites which can be studied by electron crystallography. Work along this line is in progress.

A critical feature of these materials is their propensity to form both intra- and intermolecular hydrogen bonds. The relative number and strength of such interactions may influence the supramolecular geometry adopted by the system. In particular, we note the different structures observed among dimer pairs, which differ only in the substitution at the nitrogen center. A methyl group results in an exclusive dimer−dimer geometry, whereas ethyl, propyl, and butyl substituents cause a twist about the central nitrogen, resulting in an extended ladder structure. These differences were first elucidated using double quantum solid-state NMR[27] and later confirmed using X-ray diffraction.[29] An unanswered question is the effect of substituents on the extended structures − both their packing geometries and their physical properties. We begin to explore possible answers in this paper, focusing on the methyl-substituted oligomers and polymer. The influence of hydrogen bonding on the structural and physical properties of the benzoxazine family can be considered in the more general category of supramolecular structures, and a particular challenge is to determine the hydrogen-bonded structure in systems whose heavy-atom structure is *not* known. Here we combine advanced solid-state NMR with advanced computational strategies to meet this challenge.

Applying fast magic-angle spinning (MAS), we have successfully demonstrated that high-resolution solid-state NMR is able to provide detailed structural information about the hydrogen-bonding arrangements in benzoxazines. Both qualitative descriptions of packing geometries, based on 2D ^{1}H double quantum (DQ) spectra,[27] and quantitative analysis of the N−H distance in the methyl benzoxazine dimer[30] derived from heteronuclear ^{1}H−^{15}N dipolar sideband patterns, have been presented. Here we demonstrate a powerful combination of solid-state NMR and DFT-based calculations, which enables us to characterize essential structural features of the methyl benzoxazine oligomers and to propose molecular structures that are based on energy minimization, hydrogen-bond measurement, and chemical-shift evaluation.

Homonuclear DQ NMR methods provide an excellent, facile route to qualitative structural evaluation, based on the proton−proton proximities evidenced in these spectra. The method relies on the generation of double quantum coherences between proximal ^{1}H spins, covering a ^{1}H−^{1}H distance range of up to approximately 3.5 Å, thereby probing the spatial arrangement of protons based on the strength of the through-space dipolar coupling.[31−34] Heteronuclear ^{1}H−^{15}N recoupled polarization transfer (REPT) is a complementary method for both correlations and quantitative distance measurements, which uses rotor-encoding of dipolar couplings via sideband patterns recorded in the indirect dimensions.[35] Other methods for heteronuclear recoupling of the dipolar coupling have been demonstrated and used for N−H distance measurements;[36,37] however, we selected REPT here for its robust performance under fast MAS conditions. An enhancement of the signal intensity provided by this method can be achieved both through the use of inverse detection[30,38] and, moreover, through the addition of spoil-gradients (G_z) at appropriate positions in the pulse sequence, as described recently by Saalwächter and Schnell.[39] This method has been successfully used to precisely measure N−H bond lengths (on the order of 110 pm) with ^{15}N in natural abundance. However, for the longer distances relevant in the benzoxazines, we were unable to excite a strong enough signal under natural abundance conditions. Therefore, the ^{15}N−^{1}H distance measurements described here were performed on a ^{15}N-enriched (>95%) methyl benzoxazine tetramer and are compared with the optimized structure.

We have performed geometry optimizations and NMR chemical shift calculations in the framework of density functional theory (DFT).[40] In recent years, it has become possible to calculate NMR chemical shifts not only for isolated molecules, but also for extended systems such as amorphous or crystalline solids and liquids. Here, we use a recently developed

(20) Monkman, A. P.; Palsson, L. O.; Higgins, R. W.; Wang, C.; Bryce, M. R.; Batsanov, A. S.; Howard, J. A. *J. Am. Chem. Soc.* **2002**, *124*, 6049−6055.
(21) Ezuhara, T.; Endo, K.; Aoyama, Y. *J. Am. Chem. Soc.* **1999**, *121*, 3279−3283.
(22) Ishida, H.; Low, H. Y. *Macromolecules* **1997**, *30*, 1099−1106.
(23) Kim, H. D.; Ishida, H. *J. Appl. Polym. Sci.* **2001**, *79*, 1207−1219.
(24) Macko, J. A.; Ishida, H. *J. Polym. Sci., Part B: Polym. Phys.* **2000**, *38*, 2687−2701.
(25) Ishida, H.; Rodriguez, Y. *Polymer* **1995**, *36*, 3151−3158.
(26) Dunkers, J.; Zarate, E. A.; Ishida, H. *J. Phys. Chem.* **1996**, *100*, 13514−13520.
(27) Schnell, I.; Brown, S. P.; Low, H. Y.; Ishida, H.; Spiess, H. W. *J. Am. Chem. Soc.* **1998**, *120*, 11784−11795.
(28) Ishida, H.; Moran, C. *Macromolecules* **1998**, *31*, 2409.
(29) Kim, H.-D.; Ishida, H. *J. Macromol. Chem. Macromol. Symp.* **2003**, accepted.
(30) Goward, G. R.; Schnell, I.; Brown, S. P.; Spiess, H. W.; Kim, H. D.; Ishida, H. *Magn. Reson. Chem.* **2001**, *39*, S5−S17.
(31) Schnell, I.; Spiess, H. W. *J. Magn. Reson.* **2001**, *151*, 153−227.
(32) Lee, Y. K.; Kurur, N. D.; Helmle, M.; Johannessen, O. G.; Nielsen, N. C.; Levitt, M. H. *Chem. Phys. Lett.* **1995**, *242*, 304−309.
(33) Brinkmann, A.; Edén, M.; Levitt, M. H. *J. Chem. Phys.* **2000**, *112*, 8539−8554.
(34) Hohwy, M.; Jakobsen, H. J.; Edén, M.; Levitt, M. H.; Nielsen, N. C. *J. Chem. Phys.* **1998**, *108*, 2686−2694.
(35) Saalwächter, K.; Graf, R.; Spiess, H. W. *J. Magn. Reson.* **2001**, *148*, 398−418.
(36) Brinkmann, A.; Levitt, M. H. *J. Chem. Phys.* **2001**, *115*, 357−384.
(37) Zhao, X.; Sudmeier, J. L.; Bachovchin, W. W.; Levitt, M. H. *J. Am. Chem. Soc.* **2001**, *123*, 11097−11098.
(38) Schnell, I.; Langer, B.; Söntjens, S. H. M.; van Genderen, M. H. P.; Sijbesma, R. P.; Spiess, H. W. *J. Magn. Reson.* **2001**, *150*, 57−70.
(39) Schnell, I.; Saalwächter, K. *J. Am. Chem. Soc.* **2002**, *124*, 10938−10939.
(40) Jones, R. O.; Gunnarsson, O. *Rev. Mod. Phys.* **1989**, *61*, 689−746.

Scheme 1. Synthesis of Model Trimer

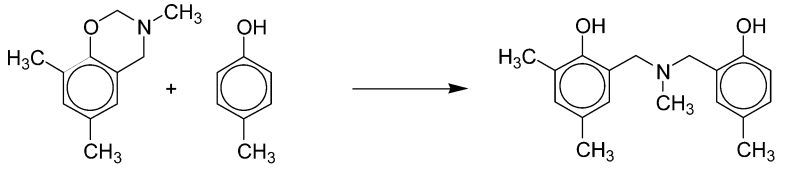

(I) (II)

(I) + (II)

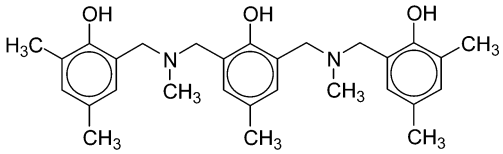

(III)

Scheme 2. Synthesis of Model Tetramer

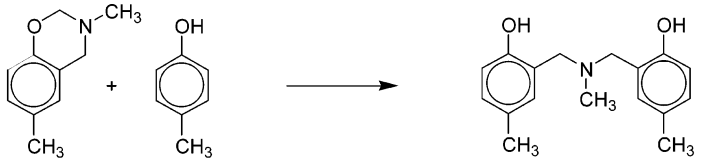

(IV) (V)

2 (I) + (V)

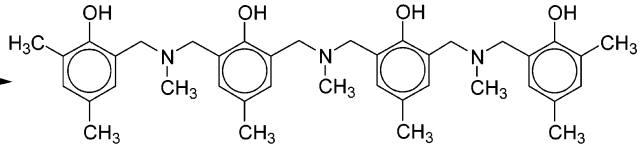

(VI)

method for extended systems[41] for the benzoxazine dimer in its crystal structure, and we use a supercell technique for the benzoxazine trimer and tetramer in vacuo.

The isolated structures of both trimer and tetramer have strong intramolecular OH···N and weak OH···O hydrogen bonds that keep them in a closed-ring like geometry. In the condensed phase, it would be further stabilized by packing effects such as van der Waals interactions between phenyl rings of neighboring molecules. However, because the material does not form large crystals, these effects are assumed to be of moderate strength. So far, there is little evidence for intermolecular hydrogen bonds, but we are currently investigating the possibility of a competing arrangement which would form ladderlike microstructures.

Experimental Section

Synthesis of 2,6-Bis[*N*-(3,5-dimethyl-2-hydroxybenzyl)-*N*-methylamino-methyl]-*p*-cresol (III, Scheme 1, Methyl-trimer). The starting monomer, 3,4-dihydro-3,6,8-trimethyl-2*H*-1,3-benzoxazine, **I**, was prepared by the procedure described by Dunkers and Ishida.[42] To obtain the intermediate dimer **II**, equimolar portions of the monomer **I** and *p*-cresol were heated at 80 °C for 12 h, and the resulting yellow product was recrystallized from *n*-hexane. This intermediate dimer **II** was reacted again with an equimolar portion of the monomer **I** without reaction solvent at 80 °C for 48 h. The resulting yellow product was cooled and was subsequently purified by column chromatography with silica gel using hexane/acetone (20:1) as the eluent. The product was fine white crystalline powder. ^{1}H NMR (200 MHz, $CDCl_3$, 298 K) δ: 2.20, 2.21 (15H, Ar−CH_3), 2.22 (6H, N−CH_3), 3.68 (8H, Ar−CH_2−N), and 6.70, 6.84, 6.86 (6H, Ar−H). ^{13}C NMR (50.1 MHz, $CDCl_3$, 298 K) δ: 15.81, 20.27 (5C, Ar−C), 40.95 (2C, N−CH_3), 58.78, 59.59 (4C, Ar−C−N), and 122.14−154.05 (18C, Ar). Anal. Calcd for $C_{29}H_{38}N_2O_3$: C, 75.29; H, 8.28; N, 6.06. Found: C, 75.09; H, 8.30; N, 6.11. Mass spectrometry (MS-FD) exp., 462.4; calcd. for $C_{29}H_{38}N_2O_3$, 462.3.

Synthesis of *N*,*N*-Bis{2-hydroxyl-5-methyl-3-[(*N*-3,5-dimethyl-2-hydroxyl-benzyl)-*N*-methylaminomethyl]}-methylamine (VI, Scheme 2, Methyl-tetramer). The model tetramer for polybenzoxazine was synthesized according to the following procedure using 2,4-dimeth-

(41) Sebastiani, D.; Parrinello, M. *J. Phys. Chem. A* **2001**, *105*, 1951−1958.

(42) Dunkers, J.; Ishida, H. *Spectrochim. Acta, Part A* **1995**, *51*, 855−867.

ylphenol, *p*-cresol, formaldehyde, and methylamine. The starting monomer, 3,4-dihydro-3,6-dimethyl-2*H*-1,3-benzoxazine, **IV**, was prepared by the procedure described by Dunkers and Ishida.[42] The intermediate dimer **V** was synthesized by heating equimolar portions of the monomer **IV** and *p*-cresol at 80 °C for 12 h, and the resulting yellow product was recrystallized from *n*-hexane. The mixture of intermediate dimer **V** and monomer **I** (1:2 mole ratio) was refluxed in chloroform for 48 h. After the reaction mixture was cooled to room temperature, chloroform was removed with a rotary evaporator, and the resulting yellow solid was subsequently purified by column chromatography with silica gel using hexane/acetone (20:1) as the eluent. ^{15}N-enriched methyl-tetramer was prepared by the same method as the methyl-tetramer with the exception of methylamine-^{15}N hydrochloride. The product was a fine white powder. ^{1}H NMR (200 MHz, $CDCl_3$, 298 K) δ: 2.19, 2.21 (18H, Ar$-CH_3$), 2.23 (9H, N$-CH_3$), 3.63, 3.66 (12H, Ar$-CH_2-$N), and 6.66, 6.84, 6.86 (8H, Ar$-$H). ^{13}C NMR (50.1 MHz, $CDCl_3$, 298 K) δ: 15.81, 20.27 (6C, Ar$-$C), 40.95 (3C, N$-CH_3$), 57.57, 58.38, 59.59 (6C, Ar$-$C$-$N), and 121.84$-$153.65 (24C, Ar). Anal. Calcd for $C_{39}H_{51}N_3O_4$: C, 74.85; H, 8.21; N, 6.71. Found: C, 74.66; H, 7.99; N, 6.84. Mass spectrometry (MS-FD) exp., 627.6; calcd. for $C_{39}H_{51}N_3O_4$ (with 100% ^{15}N isotope), 628.4.

NMR Methods. All experiments were carried out on a Bruker Avance 700 solid-state NMR spectrometer running at Larmor frequencies of 700.13 and 70.93 MHz for ^{1}H and ^{15}N, respectively. The measurements were performed using a 2.5 mm MAS probe with typical rotor frequencies of 30 kHz, $\pi/2$ pulse lengths of 2$-$2.5 μs for both ^{15}N and ^{1}H pulses, and recycle delays of 2 s. ^{1}H double-quantum experiments were performed using the compensated BaBa pulse sequence.[31] The heteronuclear recoupling sequence used to probe dipolar couplings was ^{15}N$-^1$H indirectly detected REPT-HDOR, with selection of the ^{1}H$-^{15}$N coupling supported by spoil gradients (G_z) of 100 μs duration and 100$-$200 G/cm strength (pulse sequence given in ref 39); rotor-encoded sideband patterns were acquired applying dipolar recoupling for 20 rotor periods (τ_r) during both excitation and reconversion. The t_1 dimension was incremented in steps of 1.67 μs (corresponding to $\tau_r/20$), and 40 t_1 slices were collected, which were subsequently catenated over 40 rotor periods prior to Fourier transformation (as described in ref 43).

Computational Details. To calculate the minimum energy geometries for all systems, we used the Car-Parrinello Molecular Dynamics simulation package, a density functional theory code based on a plane wave representation of the electronic structure.[44] Because of its known ability to reproduce reliably the character and strength of hydrogen bonds, the Becke$-$Lee$-$Yang$-$Parr (BLYP)[45] exchange-correlation functional was used, together with Goedecker-type pseudopotentials.[46] A plane wave cutoff of 70 Ry was chosen for all calculations, and the sampling of the Brillouin zone was restricted to the Γ-point. In all systems, the atomic positions were subsequently optimized until the maximum component of the energy gradient dropped below 5×10^{-4} au.

As the starting point for the benzoxazine dimer, we used the known crystal structure.[26] The geometry optimization was performed under periodic boundary conditions, taking into account the monoclinic crystal lattice. For the isolated benzoxazine trimer and tetramer molecules, we started from geometries generated by simulated annealing calculations with a standard all-atom force-field using point charges fitted by the restricted electrostatic potential method (RESP).[47] All atoms were subsequently relaxed at the DFT/BLYP level of theory in a sufficiently large unit cell to simulate isolated molecules. The simulation boxes were chosen such as to leave a distance of approximately 5 Å of empty space between the molecules to exclude interactions between its images in neighboring cells. Possibilities for packing effects are the focus of ongoing simulations and will be presented in a further work. The use of simulated annealing with molecular dynamics can be more efficient than a standard geometry optimization. Further, an MD simulation shows less tendency to get stuck in a local minimum or a saddle point of the potential energy surface, thus avoiding the necessity of performing a calculation of the second derivatives.

A recently developed method for calculating NMR chemical shielding tensors in DFT under periodic boundary conditions[41] that is implemented in CPMD was used to obtain the NMR resonance frequencies. It bears some resemblance to the IGLO approach,[48] but is actually a variant of the CSGT formulation[49] extended to periodic systems in a pseudopotential plane wave formulation.[44] The method has been shown to yield a very good agreement with experiment, in particular, concerning the effects of hydrogen bonding.[50$-$52] To compare to experimental results, the shieldings were referenced to tetramethylsilane (TMS) according to $\delta(\mathrm{H}) = \sigma(\mathrm{TMS}) - \sigma(\mathrm{H})$ with σ(TMS) being the shielding calculated for an isolated TMS molecule at the same level of theory. A Gaussian broadening with a half-width of 0.15 ppm was applied to the individual proton shift values, yielding the spectra shown below.

We estimate the error in the DFT calculation of the chemical shieldings to be in the range of about $\pm$0.5 ppm. It has two independent origins. First, the description by DFT as such can give rise to a maximum deviation of $\pm$0.5 ppm in the NMR parameters, when compared to quasi-exact methods such as coupled-cluster approaches. In most situations, however, relative shifts and trends are much better reproduced. The second origin is the geometry obtained from the DFT energy minimization, which does not include finite temperature effects and can thus be intrinsically wrong by about 0.05 Å. With a typical slope of 5 ppm/Å for ^{1}H shifts as a function of its location within a hydrogen bond, the geometric error could lead to a shift deviation of another $\pm$0.3 ppm.

For all calculations, we used a self-built Beowulf-cluster of 16 Pentium-4 machines with a MyriNet interconnect, running under the Linux operating system. The computational time was typically 1000$-$2000 processor-hours per system for the geometry optimization and the NMR calculations. This corresponds to a big total of roughly 10^{16} floating point operations.

Results and Discussion

Figure 1 shows the DFT/BLYP-optimized structures of the methyl benzoxazine trimer and tetramer together with the paired-dimer structure.[26] While the dimer forms pairs of molecules through *inter*molecular hydrogen bonding, the trimer and tetramer exhibit *intra*molecular hydrogen bonding, such that a single oligomer is self-contained in its geometry. Supporting data from solution state IR dilution studies show that, in both the trimer and the tetramer, the hydrogen bonds persist unchanged even in extremely dilute solution and are thus attributed to *intra*molecular hydrogen bonds.[29] The question then arises whether these structures are also present in the solid, where packing effects can lead to the formation of ladder-type arrangements, based on both intra- and intermolecular H-bonds.[27,29]

(43) Saalwächter, K.; Spiess, H. W. *J. Chem. Phys.* **2001**, *114*, 5707$-$5728.
(44) Hutter, J.; Ballone, P.; Bernasconi, M.; Focher, P.; Fois, E.; Goedecher, S.; Parrinello, M.; Tucherman, M. CPMD Computer Code, 1995, MPI für Festkörperforschung, Stuttgart, Germany, and IBM Zürich Research Lab.
(45) (a) Becke, A. D. *Phys. Rev. A* **1988**, *38*, 3098. (b) Lee, C.; Yang, W.; Parr, R. G. *Phys. Rev. B* **1988**, *37*, 785.
(46) Goedecker, S.; Teter, M.; Hutter, J. *Phys. Rev. B* **1996**, *54*, 1703$-$1710.
(47) Bayly, C. I.; Cieplak, P.; Cornell, W. D.; Kollman, P. A. *J. Phys. Chem.* **1993**, *97*, 10269$-$10280.
(48) Kutzelnigg, W. *Isr. J. Chem.* **1980**, *19*, 193$-$200.
(49) Keith, T. A.; Bader, R. F. W. *Chem. Phys. Lett.* **1993**, *210*, 223$-$231.
(50) Sebastiani, D.; Goward, G.; Schnell, I.; Parrinello, M. *Comput. Phys. Commun.* **2002**, *147*, 707$-$710.
(51) Sebastiani, D.; Parrinello, M. *ChemPhysChem* **2002**, *3*, 675$-$679.
(52) Goward, G. R.; Schuster, M. F. H.; Sebastiani, D.; Schnell, I.; Spiess, H. W. *J. Phys. Chem. B* **2002**, *106*, 9322$-$9334.

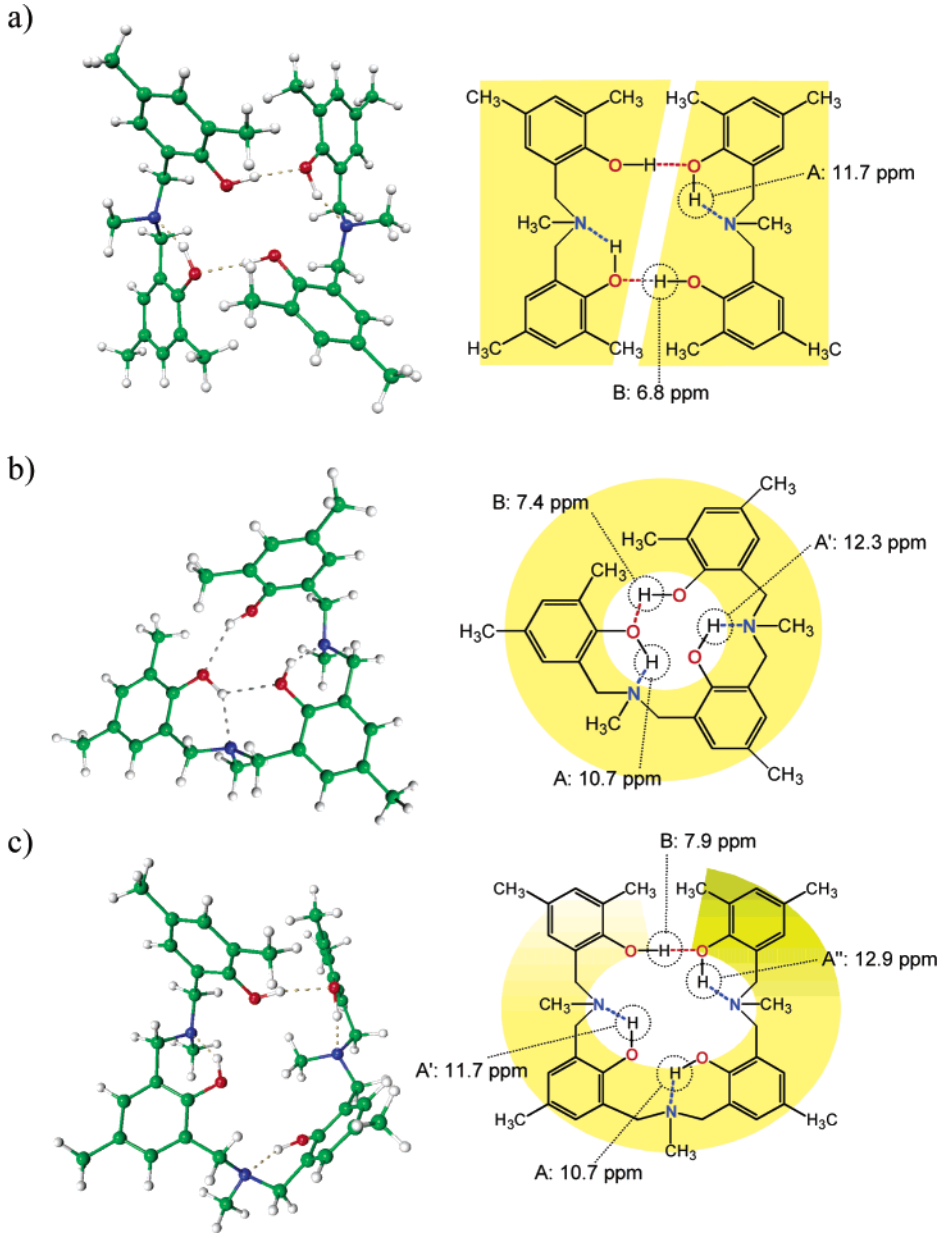

Figure 1. Methyl benzoxazine dimer, trimer, and tetramer structures in their ab initio optimized geometries. The dimer (a) forms pairs of molecules via double intermolecular N−H···O···H−O hydrogen bonds. The trimer structure (b) comprises a nearly planar ring, while in the tetramer, (c), the fourth monomer unit overlaps the start of the ring geometry, depicting the beginning of a helix. The experimental ^{1}H chemical shifts are assigned to the protons forming hydrogen bonds.

A comparison of the experimental ^{1}H MAS NMR spectra and the calculated ^{1}H NMR spectra is given in Figure 2. The latter were obtained from DFT-based calculations of a periodic structure built up from the models shown in Figure 1, while the MAS spectra were obtained from 10 mg of each sample, packed in a 2.5 mm rotor which was spun at 30 kHz. First, we consider the experimental ^{1}H MAS NMR spectra of the series of oligomers, the top traces in Figure 2. The spectra are interpreted according to an alphabetical assignment, beginning with the H-bonded resonances. N−H's at the highest resonance frequency are labeled "A" and differentiated with primes for increasing number of resolved N−H resonances. O−H's are labeled "B", aromatic resonances are labeled "C,D", and aliphatic resonances are labeled "E,F". Qualitatively, it is evident that the hydrogen-bonding structures are different for the dimer, trimer, and tetramer. The clearest difference among the spectra is the increasing number of resolved N−H resonances with increasing oligomer length, from one to two, to three. The chemical shifts are listed in Table 1. The N−H resonances begin at 11.7 ppm in the dimer and spread around this central frequency, as more resonances are added in the oligomers. Considering the O−H resonances, we see in this case a trend toward higher resonance frequency with increasing oligomer length.

The agreement between the experimental and calculated spectra is striking. Most satisfying is the correlation between the number and position of the resonances in the N−H region (10−15 ppm). In the dimer, only one N−H resonance is determined at 11.7 and 12.2 ppm by experiment and calculation, respectively. In addition, the dimer's O−H resonance is found at 6.9 ppm experimentally and at 7.0 ppm by calculation. In the trimer, two N−H resonances are found, at 10.7 and 12.3

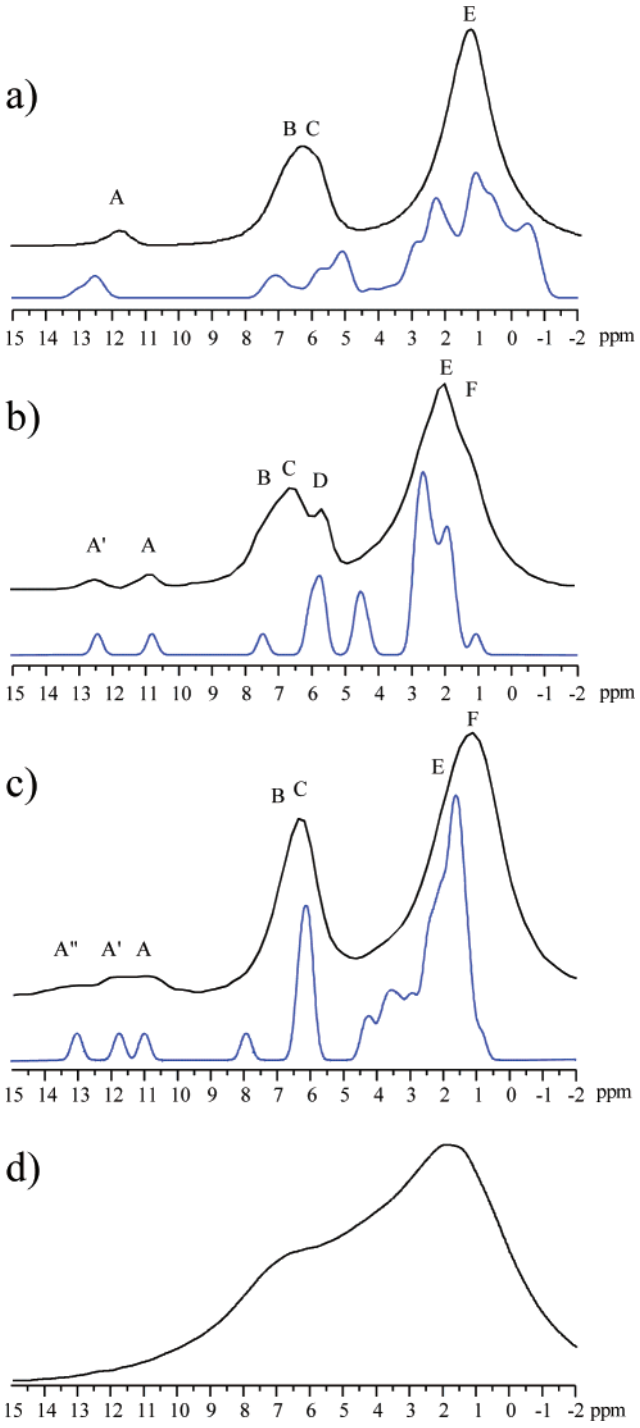

Figure 2. Comparison of calculated (blue) and experimental ^{1}H MAS NMR spectra for the dimer (a), trimer (b), and tetramer (c). ^{1}H DQ MAS spectrum of cross-linked polybenzoxazine based on methylamine (d). Resolved resonances are labeled according to the following pattern; A, N−H protons; B, O−H protons; C,D, aromatic protons; E,F, aliphatic protons. A, A′, and A″ indicate the increasing number of N−H resonances observed with increasing oligomer length.

ppm in the experimental spectrum and at 10.7 and 12.2 ppm in the calculated spectrum. In contrast, the tetramer shows three N−H resonances in both experimental and calculated spectra, in the range from 10.0 to 13.5 ppm. The reduced resolution in the experimental spectrum of the tetramer demonstrates that the material is not as highly ordered as the trimer. Nevertheless, on the basis of the similarity between our experimental and calculated data, we are confident in the validity of the three-dimensional structural conformations proposed. Further support for these molecular geometries is found in the 2D homonuclear DQ NMR spectra of the materials, discussed below.

Table 1. Calculated and Experimental ^{1}H Chemical Shifts of Benxoxazine Dimer, Trimer, and Tetramer[a]

chemical shifts in ppm	N–H resonances A″	A′	A	O–H B	aromatic C	aromatic D	aliphatic E	aliphatic F
dimer, expt.			11.7	6.8	6.5−5.5	N/A	3−0 ppm	N/A
dimer, calc.			12.2	7.0	6.0−5.0	N/A	3−0 ppm	N/A
trimer, expt.		12.3	10.7	7.4	7.0−5.0	6.0−5.5	3.0−1.5	1.5−1.0
trimer, calc.		12.2	10.7	7.4	6.2−5.5	4.8−4.2	3.0−1.5	1.5−1.0
tetramer, expt.	12.9	11.7	10.9	7.9	7.2−5.5	N/A	3.5−1.0	2.0−0.0
tetramer, calc.	13.1	11.8	11.1	7.0	6.5−5.8	N/A	4.2−2.0	2.0−0.5

[a] We note that the spectral resolution within the aromatic and aliphatic regions is poor, due to significant overlap, and thus ranges of resonance frequencies are given.

To investigate the relative strength of the intramolecular hydrogen bonds in more detail, we have performed further calculations on the benzoxazine trimer and tetramer. First, the OH···O hydrogen bond that is responsible for the ring closure was opened by imposing an O···O distance of about 3 Å, while allowing the rest of the molecule to relax completely. This resulted in an increase in total energy of 10−12 kJ/mol for both molecules. Furthermore, a variety of alternative geometries were generated with the combined force-field and DFT geometry optimization approach. In all alternative geometries, the OH···N intramolecular hydrogen bonds remained intact, thus always imposing an internal curvature on the molecule. The outer OH···O bond was conserved in the majority of the structures obtained, yielding approximately the same overall geometry and a similar NMR pattern. In the cases where the ring-closing did not take place, other OH···O bonds were formed, but the total energies of the systems were always more than 25 kJ/mol higher than that in the helical arrangement. In addition, the calculated NMR spectra showed no resemblance to the experimentally observed spectrum. Thus, there is conclusive evidence that the trimer and tetramer form ring-shaped and helical structures, respectively, which are held together by a sufficiently strong intramolecular OH···O hydrogen bond.

With respect to the dimer, we need to add that the result of the geometry optimization of the periodic structure resulted in a N−H distance of 1.70 Å, which is significantly shorter than the previously determined value of (1.96 ± 0.05) Å.[30] Remarkably, the chemical shift of the NH proton occurs at 11.7 ppm in the nonlabeled sample (spectrum shown in Figure 2), which differs from that observed at 11.2 ppm in both the labeled material on which the distance measurement was made and a previously prepared sample.[27,30] We also note that the sample examined in ref 27 was not uniform, but also contained a fraction of the ladder-type packing arrangement, as was observed in the 2D ^{1}H DQ spectrum of that material. Therefore, we attribute the difference not to an inaccuracy in the measurement or the geometry optimization, but rather to an imperfect crystal packing, which results in the longer-than-optimal N−H distance. This conclusion is based primarily on the extreme sensitivity of the proton chemical shift to the NH distance. To test this hypothesis, a NH distance was fixed, and the geometry optimization was performed under the constraint of 1.9 Å. The energy difference per dimer pair (i.e., 4 H-bonds) was small, approximately 3 kJ/mol, and the resulting ^{1}H chemical shift for the NH resonance was less than 11 ppm, in agreement with the

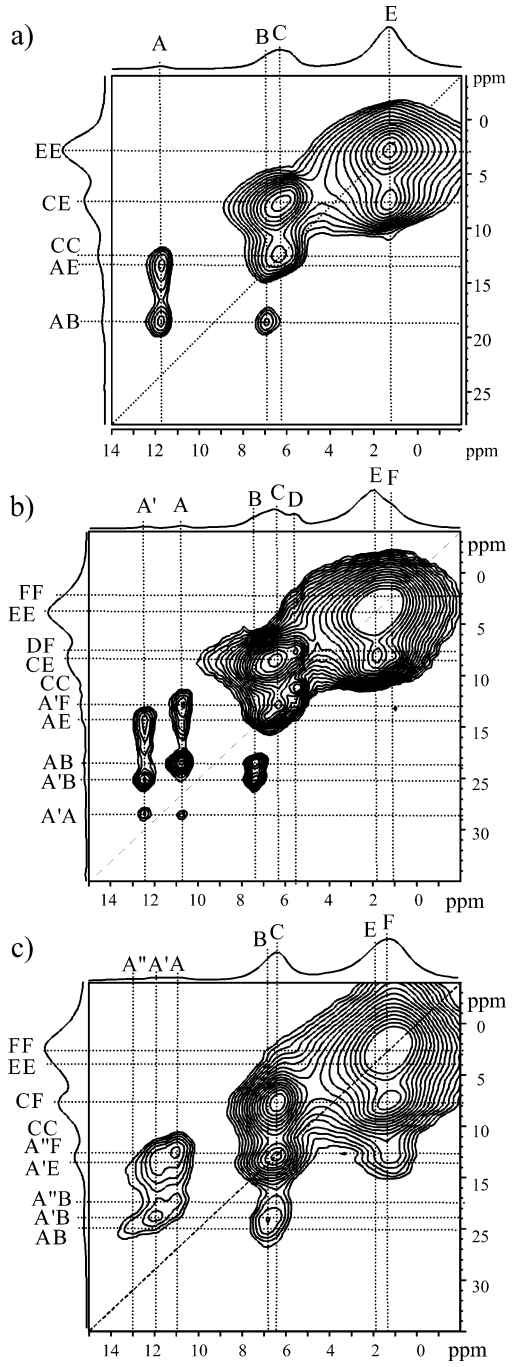

Figure 3. ^{1}H 2D DQ NMR spectra for the dimer (a), trimer (b), and tetramer (c), obtained at ambient temperature, under 30 kHz MAS with one rotor period of dipolar recoupling. $\pi/2$ pulse lengths of 2 μs and recycle delays of 2 s were implemented. Sixty-four transients were averaged for each of 32 slices acquired in the indirect dimension. Labels correspond to those used in Figure 2.

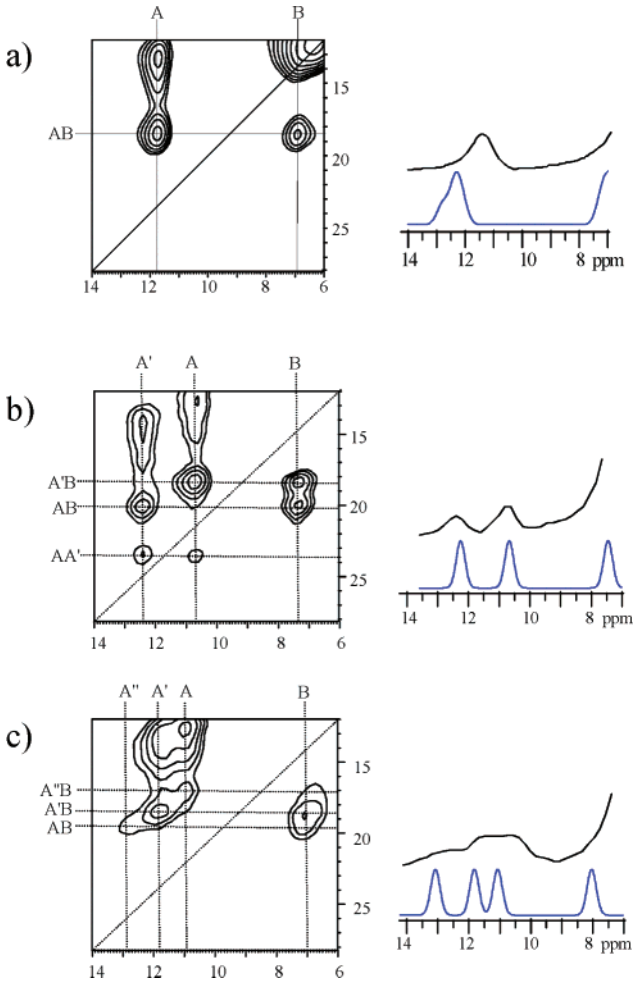

Figure 4. Regions of the ^{1}H 2D DQ NMR spectra (shown in Figure 2) relevant for the hydrogen bonds of the dimer (a), trimer (b), and the tetramer (c). On the right, experimental spectra are compared to calculated ^{1}H shifts (blue).

trend we describe. Apparently, the position of the N−H can be adjusted to cope with packing requirements. At this point, we return to considering the trimer and tetramer structures, which are the primary focus of this paper.

The 2D ^{1}H−^{1}H DQ NMR spectra obtained for the dimer, trimer, and tetramer are shown in Figure 3. The reader is referred to previous publications for analogous spectra obtained for the methyl dimer.[27,30] As in the case of the dimer, strong resonances in the alphatic and aromatic regions are observed as expected along the diagonal of the 2D spectrum and arise from self-correlations of like methyl (E), methylene (F), and phenyl protons (C and D) in both oligomers. As well, various contacts are observed between the resonances C, D, E, and F, all of which, however, are of no significance with respect to the hydrogen-bonding scheme, but merely reflect proton−proton proximities that are obvious from the molecular structure.

More significant in terms of probing the structures are the correlations among the hydrogen-bonded protons, whose resonances occur in the lower left quadrant of the DQ spectrum. An expansion of this region is given in Figure 4. The OH resonances, labeled B, are evident in all three spectra, at 6.9 ppm in the dimer, 7.4 ppm in the trimer, and 8.0 ppm in the tetramer. The N−H resonances, labeled A in the dimer, A and A′ in the trimer, and A, A′, and A″ in the tetramer, distinguish the oligomers both molecularly, in the number of N−H resonances present, and structurally, in the nature of the correlations present. In the methyl benzoxazine dimer, trimer, and tetramer, one, two, and three N−H resonances, respectively, are observed. However, none of these N−H protons shows an "auto" correlation of the type A−A, A′−A′, or A″−A″, which means that the N−H protons are spatially separated from each other. For the trimer, however, a correlation between A and A′ is found at 23.8 ppm in the DQ dimension, which indicates that these two NH protons are in close proximity to each other

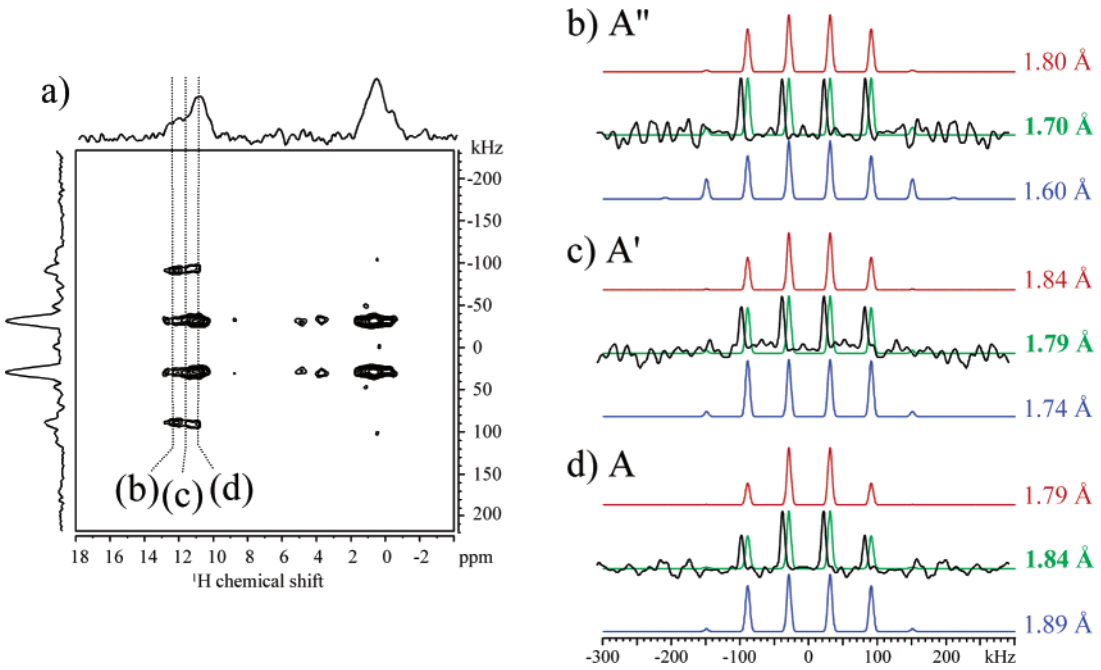

Figure 5. (a) $^{15}N-^{1}H$ inverse CP-REPT-HDOR spectra for the benzoxazine tetramer with ^{15}N enrichment, collected using $\tau_{exc} = 20\ \tau_r$ under MAS at 30 kHz. The experimental 1D patterns shown in (b, c, d) were taken from the 2D spectrum shown in (a) at the resonance positions of the NH protons A″, A′, and A, respectively. The colored patterns in (b, c, d) are calculated using the N−H distances given on the right. The red and blue patterns represent the upper and lower limits of the error margin, while the green pattern fits best to the experimental data.

in the ring structure. In contrast, in the spectrum of the tetramer, no such A−A′ or A−A″ contacts are observed, which is consistent with an increase in the spatial separation between the nitrogens in the larger oligomer. The A−B correlations present in all spectra are consistent with intramolecular contacts between the protons in the two types of hydrogen-bonded (N−H and O−H) protons. Similarly, expected contacts between the NH resonances and the methyl protons of the methyl at the amine position are always present.

These data are in good agreement with the molecular conformations illustrated in Figure 1. In particular, the quasi-planar ring-shaped geometry of the trimer brings the NH protons into spatial proximity with each other and is consistent with the observed A−A′ contact. The respective proton−proton distance in the molecular DFT model is 2.74 Å. Furthermore, the quasi-helical tetramer structure occupies comparatively more free volume, such that the N−H protons are separated from each other by greater than 4.0 Å and therefore fall outside the range of H−H distances observable via DQ NMR under these conditions.[27,31]

A ^{1}H 1D DQ MAS spectrum obtained for cross-linked, high molecular weight polybenzoxazine based on methylamine is shown in Figure 2d and clearly does not afford sufficient spectral resolution for a full structure determination due to the overlap among different types of hydrogen-bonded resonances, and generally broadened spectral features. The trend toward an increasingly complex hydrogen-bonding structure, with individually resolved resonance lines observed for the small oligomers, accounts for the broad ^{1}H resonances observed in the polymer, where a superposition of spectra for different H-bonded structures is expected.

Turning to the chemical properties of the polybenzoxazine polymers, we find supporting evidence for the structures described here. The overlapped ring geometry of the tetramer leads us to hypothesize a helical geometry as the most likely conformation of the polymer. In such a geometry, the hydrogen bonds are found on the inner side of the helix, where they are protected from chemical attack. Such a geometry is consistent with the properties such as lack of water absorption and lack of contraction or expansion upon curing, the industrially favorable properties of these polymers.

$^{15}N-^{1}H$ Distance Measurements. In our previous investigation of the N−H···O distance in the methyl benzoxazine dimer, a distance of (1.96 ± 0.05) Å was measured in the ^{15}N-labeled sample prepared for that study. Here, we present distance measurements for the N−H contacts in the ^{15}N-labeled tetramer, using an improved variant of the pulse sequence.[39] The new pulse sequence again makes use of ^{1}H detection, with the added advantage of pulsed field gradients (PFGs), or, alternatively, ^{1}H R^3 pulses, which dephase unwanted ^{1}H magnetization. The measurements of N−H distances in the tetramer are in good agreement with the calculated structure. Figure 5 shows the rotor-encoded $^{1}H-^{15}N$ dipolar sideband pattern (Figure 5a), together with the 1D patterns taken from the respective regions of the 2D spectrum and corresponding calculated patterns (Figure 5b−d). We note that, while three $^{1}H(N)$ resonances could clearly be resolved in the ^{1}H MAS and DQ spectra, the resolution in the ^{1}H dimension of the sideband experiment is somewhat hampered due to the poorer signal-to-noise which results from the extremely long recoupling time required to generate the higher order sidebands necessary for accurate measurements of these relatively long distances. Therefore, the sideband patterns (in the F_1 dimension) have been extracted from the 2D spectrum at exactly those ^{1}H resonance positions (in the F_2 dimension) which are known from the ^{1}H MAS experiment. A comparison with calculated sideband patterns (colored patterns in Figure 5b−d) yields N−H distances of (1.84 ± 0.05), (1.79 ± 0.05), and (1.70 ± 0.10) Å for the NH protons A, A′, and A″, respectively. In Figure 5b−d, the red and blue patterns represent the upper and lower limits of the error margin,

while the green pattern fits best to the experimental data. The measured distances are in excellent agreement with the values found in the optimized geometry of the tetramer, that is, 1.89, 1.78, and 1.72 Å, and also concur with the calculated and experimental ^{1}H chemical shifts of the respective protons. The longest N−H distance is found for proton A, which has the smallest chemical shift (at 10.7 ppm) and forms a hydrogen bond to the central N-atom in the tetramer. The relative weakness of the hydrogen bond indicates that the central part of the tetramer experiences the most strain due to the helical geometry. For the two other NH-protons, A′ and A″, shorter N−H distances as well as larger chemical shifts (of 11.7 and 12.9 ppm) are found. These observations correspond to stronger hydrogen bonds, suggesting that the more peripheral parts of the tetramer experience less conformational strain. These data therefore confirm our proposed structure of the tetramer − the first twist of a helix.

The trend to shorter N−H distances with increasing proton resonance frequency also supports our earlier discussion of the N−H distances in the slightly differing structures of the benzoxazine dimer, where the experimentally measured N−H distance of greater than 1.9 Å correlated to a ^{1}H resonance frequency of 11.2 ppm, whereas the distance of 1.7 Å determined via geometry optimization correlated to the calculated resonance frequency of 12.4 ppm. These data show the extreme sensitivity of the ^{1}H chemical shift to its environment − particularly in the presence of hydrogen bonding. Moreover, the differences noted among the dimer samples in the solid state were undetectable by other analysis methods including solution-state NMR and FT-IR. Solid-state NMR is particularly suited to detect fine-tuning of structures via the adjustment of the NH···O hydrogen bond.

Conclusions

In summary, we have presented a case study in which the accord between DFT-based chemical shift calculations and high-resolution solid-state ^{1}H MAS NMR spectra provides ample confirmation of a supramolecular hydrogen-bonding structure. Moreover, we have established a structural motif for the methyl benzoxazine trimer and tetramer, which, in contrast to the methyl dimer pairs, are characterized exclusively by intramolecular hydrogen bonds. Extrapolating from the trends found among these oligomers, we conclude that the polybenzoxazines form helices in the solid state: such a structural conformation accounts for their favorable chemical properties.

In conclusion, this study demonstrates the remarkable success of the combination of cutting-edge experimental and computational NMR methods in the investigation of structural driving forces of supramolecular hydrogen-bonded systems.

Acknowledgment. H.I. acknowledges support from the von Humboldt Fellowship program. G.R.G. is grateful to NSERC (Canada) for support in the form of a postdoctoral fellowship. Financial support through the Deutsche Forschungsgemeinschaft (SFB 625 in Mainz) is gratefully acknowledged. We thank M. Hehn and H. Raich for their technical expertise and patience required to modify the 2.5 mm probe to incorporate gradients.

JA029059R